Journal of Korean Powder Metallurgy Institute
Vol. 5, No. 3, 1998

Selective Laser Sintering of Alumina Using an Inorganic Binder Monoclinic HBO_2 and Post-Processing

In Sup Lee
Dept. of Materials Engineering, Dongeui University,
24 Gaya-Dong, Pusanjin-Ku, Pusan, Korea 614-714
(Received August 24, 1998)

Abstract A new low melting inorganic binder, monoclinic HBO_2, has been developed for Sclective Laser Sintering (SLS) of alumina powder by dehydration process of boron oxide powder in a vacuum oven at 120℃. It led to better green SLS parts and higher bend strength for green and fired parts compared to other inorganic binders such as aluminum and ammmonium phosphate. This appeared to be due to its low viscosity and better wettability of the alumina particle surface. A low density single phase ceramic, aluminum borate ($Al_{18}B_4O_{33}$), and multiphase ceramic composites, Al_2O_3-$Al_4B_2O_9$, were successfully developed by laser processing of alumina-monoclinic HBO_2 powder blends followed by post-thermal processing; both $Al_{18}B_4O_{33}$ and $Al_4B_2O_9$ have whisker-like grains. The physical and mechanical properties of these SLS-processed ceramic parts were correlated to the materials and processing parameters. Further densification of the Al_2O_3-$Al_4B_2O_9$ ceramic composites was carried out by infiltration of colloidal silica, and chromic acid into these porous SLS parts followed by heat-treatment at high temperature (1,600℃). The densities obtained after infiltration and subsequent firing were between 75 and 80% of the theoretical densities. The bend strengths are between 15 and 33 MPa.

1. Introduction

Solid Freeform Fabrication (SFF) is an advanced manufacturing technology which generates geometrical objects directly from a three-dimensional computer image without part-specific tooling or human intervention.[1] These SFF techniques have recently been developed to overcome some of the barriers of conventional manufacturing techniques, such as difficulties in tooling complex-shaped ceramic parts and long production time in fabricating prototypes. Selective Laser Sintering (SLS) is a form of SFF and employs a focused laser beam which is controlled by a CAD data base to selectively scan a powder bed and to bind loose powder, so as to make a thin layer of bonded powder. The sintered layer is lowered from the sintering plane and a new layer of the powder is spread again. The laser scans again, resulting in both sintering of the powder particles and bonding the present layer to the underlying previous layer. The desired object is generated by laying down a number of such layers and successively sintering them.[2] The overall schematic of the SLS process is shown in Fig. 1.[3] The primary advantage of the SLS process is the flexibility of selecting the material systems compared to other SFF techniques.[4]

The two-phase powder approach to SLS, which involves binding high temperature ceramics such as alumina and silicon carbide with a low melting inor-

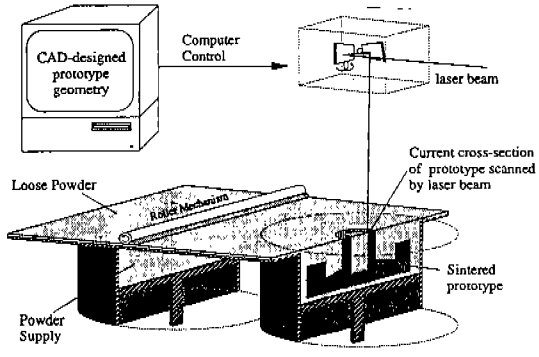

Fig. 1. Schematic representation of a SLS system.

ganic binder, is a promising technology to fabricate ceramic composite parts.[5-7] The selection of an optimum material systems for this approach depends on material properties such as a melting point of the binder material and interparticle wetting between the components in the composite powder blend.[8]

In a suitably chosen system, the low melting phase melts completely or partially under the laser beam and binds the high melting phase particles. Furthermore, it can react in some cases with the high melting phase or with the atmosphere. Further reaction can also takes place in a subsequent heating step. As a result, either another compound may incorporate into the matrix or a single phase compound may result.

The first advantage of this two-phase powder approach is an immediate access to the conventional low temperature SLS equipment for processing of high melting ceramic and metal powders without requiring the high temperature station. The second one is the possibility to avoid balling problem, which is frequently observed in the SLS process of single phase metal powders such as lead, zinc or tin.[9] When the laser beam selectively scans the powder bed, the molten particles coalesce into a sphere rather than wet the solid particles. The diameter of the sphere is about the same as that of the laser beam. This phenomenon is referred to as "balling".[10] The third one is the capability to introduce a second phase such as intermetallics and compounds into the matrix or to synthesize a new single phase if the material system is relevantly selected.

It is well known that the role of boron oxide in borosilicate glasses is to reduce the thermal expansion coefficient and to improve workability by decreasing the viscosity.[11] The low viscosity of boron oxide is attributed to its linked-ring structure, since there is a high probability that the bonds between rings are more susceptible to failure than the bonds within the rings.[12]

Especially, the selection of boron oxide as an inorganic binder is attractive for the SLS of an alumina-

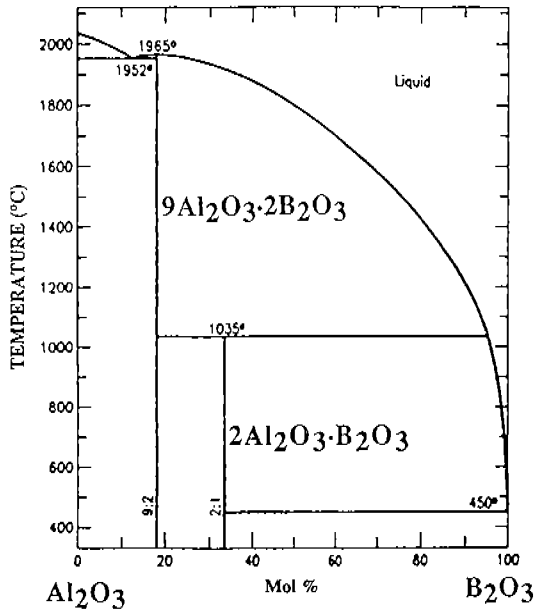

Fig. 2. Al_2O_3-B_2O_3 Phase Diagram.

boron oxide composite system because boron oxide has a low melting point (450℃) and the liquid generated due to the local melting of B_2O_3 powder during laser beam irradiation can aid the sintering process. In addition, the molten boron oxide completely envelops the neighboring solid alumina particles due to its low viscosity and better wetting. A better wetting of solid alumina powder by molten boron oxide can further enhance densification process.[5]

There are two stable crystalline compounds in the Al_2O_3-B_2O_3 system as seen in the phase diagram (Fig. 2).[13] One is $9Al_2O_3 \cdot 2B_2O_3$, the other is $2Al_2O_3 \cdot B_2O_3$. Both the compounds have orthorhombic crystal structure. Even though the melting point of $9Al_2O_3 \cdot 2B_2O_3$ is 1,950℃ according to the phase diagram, it is somewhat unstable above 1,500℃ due to the vaporization of B_2O_3. The melting point of $2Al_2O_3 \cdot B_2O_3$ is 1,035℃. It is likely that the SLS of the Al_2O_3-B_2O_3 powder blend can offer the possibility of incorporating compounds into the alumina matrix or of generating a single phase if the composition is suitably selected.

However, there is a disadvantage of boron oxide as an inorganic binder for the SLS of alumina.

Direct use of boron oxide as a low temperature phase for the SLS of alumina with a powder bed heating around 80℃ causes a weak cake through the whole powder bed during the SLS process. The cake paralyzes the powder delivery and leveling system. The main reason for this phenomenon is attributed to the formation of boric acid (H_3BO_3) due to its much lower melting point (170℃) in comparison to boron oxide (450℃). In order to overcome this barrier, phase transformation of boron oxide into various metaboric acid HBO_2 by dehydration process has been carried out. The selection of one of metaboric acid HBO_2 as a binder instead of boron oxide for SLS of alumina might solve that problem.

The samples made by SLS and simple post-thermal processing of alumina-boron oxide composite system had only about 35~40% of theoretical density due to a lower powder bed density arising from a lower apparent density (34% of theoretical density) of 15 μm alumina powder. This resulted in poor bend strengths (around 8 MPa) of the test bars. Therefore, it was necessary to increase the density for functional applications of SLS parts. Infiltration with colloids and solutions into porous SLS parts is an attractive option to increase the density.[14]

The infiltration technique densifies a porous material by filling or partially filling the interconnected porosity of a particular compact with a liquid, melt, or vapor.[15] Infiltration can incorporate additional phases into a body that is formed by well-established techniques such as pressing, extrusion, tape casting, slip casting, and injection molding. Furthermore, infiltration may provide a uniform mixing of various phases. During subsequent heat treatment of a porous powder compact infiltrated with a suitable liquid infiltrant, processes such as decomposition of infiltrant, solid-state reaction, liquid phase formation, and densification can take place depending on the system.[16]

Infiltrants such as colloidal silica, and chromic acid were selected for densification of alumina-aluminum borate ($2Al_2O_3 \cdot B_2O_3$) composites that were fabricated by firing green SLS parts, obtained from alumina-25 wt.% boron oxide powder blend, at 900℃ for 6 hours.

This paper presents (1) the experimental procedure related to the development of a new inorganic binder, monoclinic HBO_2, for SLS application, (2) the synthesis of a single phase ceramic or multiphase ceramic composites by laser processing of alumina-monoclinic HBO_2 powder blends followed by post-thermal processing, and (3) further densification of the composites by infiltration of colloidal silica and chromic acid into these porous SLS parts followed by heat-treatment at higher temperature (1,600℃). The roles of materials as well as laser and processing parameters on the mechanical and microstructural properties of the green and post-processed SLS parts are discussed.

2. Materials and Experimental Procedure

High purity alumina (melting point 2,050℃) was chosen as a high melting component since it is one of the most widely used advanced ceramics and is relatively low in cost in comparison to other high temperature ceramic materials. Boron oxide (melting point 450℃) was selected as a starting low melting phase.

For this research, aluminum oxide powder of 15 μm diameter with high purity of electronic grade provided by Norton Materials Corporation and 60 mesh (250 μm) 99% boron oxide powder from Johnson Matthey were the starting materials. The above boron oxide powder was further ground using a Szegvari attritor system and sieved to less than 75 μm.

Alumina and boron oxide powders were mixed in the ratio of 3 : 1 (25 wt.% B_2O_3), 4 : 1 (20 wt.% B_2O_3), and 5.65 : 1 (15 wt.% B_2O_3) by weight. Each powder mixture was baked out in a vacuum oven at 120℃ for 30 hours. This pre-thermal treatment caused the powder blends to form weak powder cakes, which

were subsequently broken and sieved. Each powder blend was analyzed by X-ray Diffraction (XRD) analysis to check the phase transformation of boron oxide to monoclinic HBO_2. If the transformation of monoclinic HBO_2 was not complete, then the baking-out process was repeated. Baked-out powder blends were immediately sintered in a SLS system at the University of Texas at Austin. Single layer tests were carried out on these powders with various laser power and scan speed to determine optimum laser operational conditions. Test specimens with dimensions $0.076 \times 0.025 \times 0.00625$ m ($3'' \times 1'' \times 0.25''$) were fabricated in an inert nitrogen environment using the operational parameters listed in Table 1.

When the SLS parts were complete, excess unsintered powder was removed by brushing off with a paint pen. The green parts were then heated to 800℃ with a heating rate of 5℃/min and then to the final heat-treatment temperature with a heating rate of 2℃/min in a $MoSi_2$ furnace. After keeping at the final heat treatment temperature for 6 hours, the parts were cooled back to 800℃ with a cooling rate of 2℃/min and then to room temperature with a cooling rate of 5℃/min.

The strengths of SLS parts in the green state as well as after firing at various temperatures for 6 hours were measured by 3-point bend test using an Instron constant displacement rate machine. Densities were obtained by use of sample dimensions and mass. Identification of phases and microstructural evolution at every step of processing was carried out by X-ray diffraction analysis and Scanning Electron Microscope (SEM).

For the infiltration study, test bars made from alumina-25 wt.% boron oxide with a laser energy density of 4.144 cal/cm^2 and fired at 900℃ for 6 hours were selected. Energy density is defined as laser power/(scan spacing × scan speed).[3] Ludox colloidal silica (grade TM), which was provided by Dupon Corporation, was infused into the test coupons. The silica content of this colloid is 50 wt.% and the average particle diameter is 22 nm. The test bars were partially immersed in a shallow pool of colloid, which could be drawn up to the top surface. When the top surface of the coupons was completely wet, the infiltration was assumed to have been completed. The infiltrated preforms were dried for a few hours in air at room temperature and then heated to 120℃ in a drying oven for several hours. After saturation through a series of infiltrations and drying, the samples were further heated to 1,600℃ for 16 hours to decompose the infiltrant and densify the body. By repeating this process, porous ceramic preforms could be brought to nearby 75% of theoretical density.

Chromic acid (H_2CrO_4) was pursued as a second infiltrant. It was prepared by dissolving water-soluble chromium trioxide (CrO_3) in distilled water in the ratio of 1 : 1 by weight. The infiltration of the fired, porous SLS parts were also carried out with liquid chromic acid (H_2CrO_4). Subsequent drying and heat treatment converted the chromic acid to Cr_2O_3. The laser processing condition of the test bars and infiltration procedures were same as those for the colloidal silica infiltration. During this experiment, two steps of heat treatment were carried out. First step was to convert the chromic acid to Cr_2O_3 at 900℃ for 2 hours and second one was to homogenize the composite body at 1,600℃ for 16 hours.

For each infiltration process, the strength of infiltrated test coupons was measured by 4-point bend tests. The role of infiltration for densification and strengthening was evaluated in terms of physical density and bend strength measurements. SEM micrographs of fracture surface were used to und-

Table 1. SLS operational parameters of alumina - boron oxide powder blends

Laser Power (W)	Bed Temperature (℃)	Scan Spacing (μm)	Layer Thickness (μm) 25~30 layers	Scan Speed (m/sec)
14~16.5	80~100	125	200~250	0.32~1.19

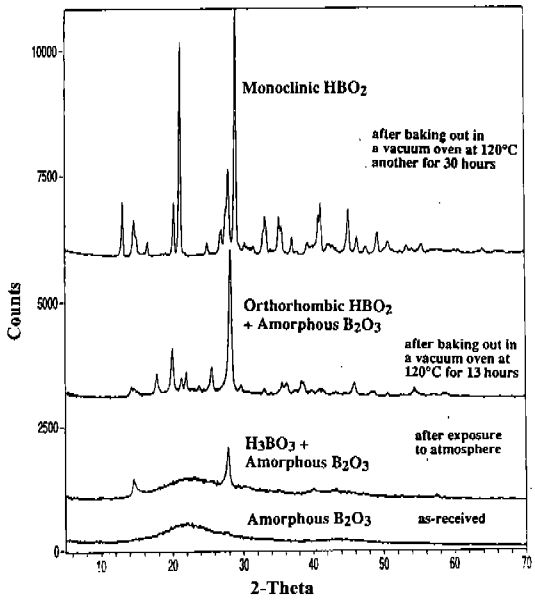

Fig. 3. X-ray diffraction patterns showing phase transformations of the initial boron oxide.

erstand further the porosity of the infiltrated parts.

3. Results and Discussion

Fig. 3 shows the phase transformation of the initial boron oxide upon reaction with atmospheric water. The as-received boron oxide is amorphous. It reacts with moisture in air and transforms into crystalline boric acid (H_3BO_3) very quickly. As a result, without baking out before laser sintering, the starting powder blend for laser sintering is a mixture of alumina, amorphous boron oxide and boric acid. Because boric acid has much lower melting point (170℃) in comparison to boron oxide (450℃), it causes a weak bed cake through the whole powder bed during SLS process with bed heating around 80℃. The cake paralyzes the powder delivery and leveling system. Without employing bed heating system, it was possible to avoid the bed caking. However, curling of the previously sintered layers takes place, making powder leveling difficult due to the displacement of those layers.

In order to overcome bed caking and curling of sintered layers, the boric acid in the initial powder blend must be removed. Furthermore, the amorphous boron oxide needs to be transformed to another phase to prevent further transformation into boric acid during SLS process, because it is too hygroscopic. It is known that dehydration of boric acid gives different forms of crystalline metaboric acid HBO_2 or boron oxide B_2O_3 depending on the baking out temperature. Table 2 shows the physical properties of various forms of metaboric acid HBO_2.[11] Therefore, conversion of the initial B_2O_3 or H_3BO_3 to HBO_2 might be an attractive solution to this problem.

Table 2. Physical properties of crystalline metaboric acid HBO_2

	CN* of B	Density (g/cm^3)	Melting Point (℃)
Orthorhombic	3	1.784	176
Monoclinic	3 and 4	2.045	201
Cubic	4	2.487	236

*CN refers to coordination number

The conversion to HBO_2 requires a partial dehydration of boric acid above 100℃ as shown in Equation 1,

$$H_3BO_3 \xrightarrow{120℃} HBO_2+H_2O \quad (1)$$

The dehydration process was carried out in a vacuum oven, manufactured by Cole-Parmer, that was connected to the housing vacuum line operating at a pressure of about 280 Torr.

The selection of the bake-out temperature was based on the experimental results. The ground and sieved (less than 75 μm) boron oxide powder, which contains some boric acid (H_3BO_3) due to exposure to air, yielded orthorhombic HBO_2 after baking out at 120℃ for 13 hours. However, the amorphous boron oxide still remained as indicated by an amorphous background in the X-ray pattern (Fig. 3). A careful dehydration of this powder at 120℃ in a rough vacuum oven for about another 30 hours and slow quenching after bake-out yielded monoclinic metaboric acid HBO_2 whose melting point is 201℃. Moreover, the amorphous B_2O_3 phase completely

transformed to monoclinic HBO_2 after this process. It seems that the amorphous boron oxide absorbs moisture and transforms to boric acid during the grinding process, which then transforms into the monoclinic HBO_2 via the orthorhombic HBO_2 during the second bake-out process. It was found that monoclinic HBO_2 avoids the bed caking phenomenon with powder bed heating temperature at 80℃ and reduces the curling problem significantly during SLS process.

Unfortunately cubic HBO_2 could not be obtained by the dehydration of boric acid (H_3BO_3). It is likely that the partial vapor pressure of boric acid inside the oven play an important role on the phase transformation. In addition, a higher bake-out temperature is needed to obtain cubic HBO_2. Further study will be required in order to understand the formation of cubic HBO_2 from boric acid through dehydration. Orthorhombic HBO_2 was determined to be too hygroscopic for SLS application; on the other hand, monoclinic HBO_2 was lightly hygroscopic since its transformation to boric acid was slow compared to orthorhombic HBO_2.

The performance of monoclinic HBO_2 as an inorganic binder for SLS of alumina was evaluated by the bend strength of the parts in the green state as well as after firing at 900℃ for 6 hours with respect to the key SLS operational parameter such as laser energy density.

The effect of binder content on bend strength of the composite (both green and after firing at 900℃ for 6 hours) is illustrated in Fig. 4. The bend strength of the composites increases as the binder content increases since all the ceramic interparticle bonds that provide the strength to the composites originate from the melting of the binder and the coating of ceramic (alumina) particles by the molten binder during laser beam irradiation. During post-thermal processing step, boron oxide reacts with alumina, resulting in aluminum borate ($2Al_2O_3 \cdot B_2O_3$) whiskers at the surface of the alumina particles. The strength of the parts fired at 900℃ for 6 hours increases as the binder content increases. This is because the higher the binder content, the more would be the aluminum borate whiskers at the surface of alumina particles and hence higher would be the strength.

The effect of laser energy density on bend strength is also shown in Fig. 4. At lower energy density, the green composites show poor strength due to insufficient melting and flowing of the binder compared to those at higher energy density where molten binder coats the ceramic particles completely as revealed by SEM. Similarly, the bend strength of fired parts fabricated with 25 and 20 wt.% boron oxide powder blends is proportional to the energy density due to an increasing local melting and flowing of the binder. As a result, at higher laser energy den-

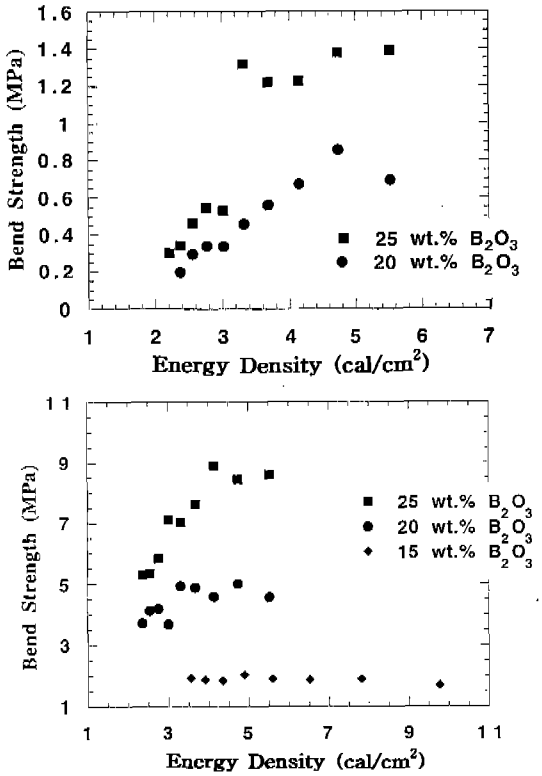

Fig. 4. (a) Bend strength of green test coupons fabricated with 15 μm alumina-boron oxide powder blends. (b) Bend strength of coupons fabricated with 15 μm alumina-boron oxide powder blends after firing at 900 ℃ for 6 hours.

sity, more ceramic particles are encapsulated by the molten binder compared to at lower energy density as revealed by SEM. Also, the green and fired part density increases as the energy density increases, which is in accordance with increasing strength with increasing energy density. However, bend strength of fired test bars made with 15 wt.% boron oxide is independent of energy density. For this system, it was required that the process be done at higher powder bed temperature (100℃) and at higher energy density in order to melt the small amount of the binder completely and bind ceramic particles together. The higher energy density used might be above the threshold energy density required to melt the whole binder thoroughly and fabricate green parts which can keep the shape. Therefore, the strength of the fired parts is independent of energy density since there is no more additional binder which will coat the ceramic particles.

Fig. 5 shows the effect of firing temperature on the mechanical and physical properties of parts fabricated with 25 wt.% boron oxide powder blends. At intermediate firing temperatures at around 800℃ ~1,100℃, the test bars show higher bend strength due to the formation of aluminum borate ($2Al_2O_3 \cdot B_2O_3$) at the surface of the alumina particles by the reaction of alumina and boron oxide at around 800℃. The morphology of $2Al_2O_3 \cdot B_2O_3$ ($Al_4B_2O_9$) was identified by SEM to be a whisker structure (Fig. 6). Below 700℃, it was found that there was no substantial reaction between alumina and boron oxide. Thus, the bend strength of the test bars fired at 550℃ is much lower than that of the samples fired at higher temperatures, even though the fired density of samples at firing temperatures up to 1,100℃ is almost similar. Therefore, the formation of whisker-like aluminum borate ($2Al_2O_3 \cdot B_2O_3$) grains at the surface of the alumina particles by the reaction between alumina and boron oxide seems to play a key role on the increase of bend strength. According to X-ray diffraction analysis, the amount of $2Al_2O_3 \cdot B_2O_3$ increases relative to that of alumina

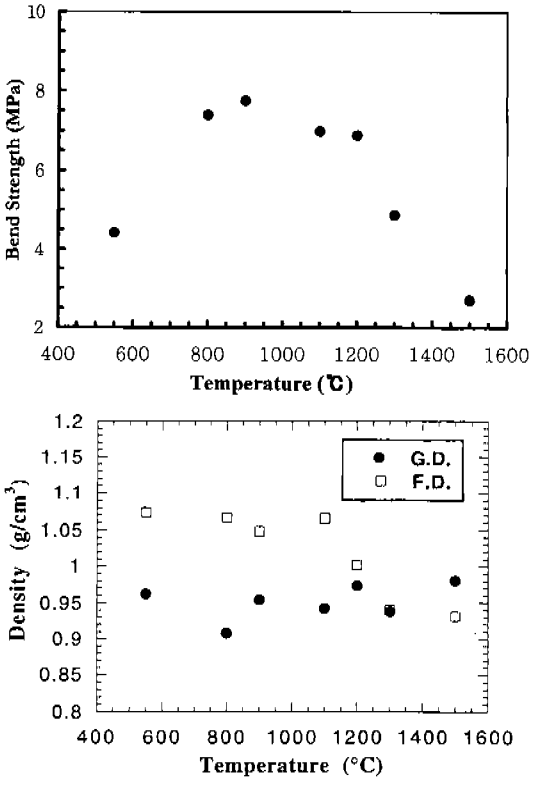

Fig. 5. (a) Effect of firing temperature on the bend strength of samples made with alumina-25 wt.% boron oxide powder blend. (b) Effect of firing temperature on the density of samples made with alumina-25 wt.% boron oxide powder blend.

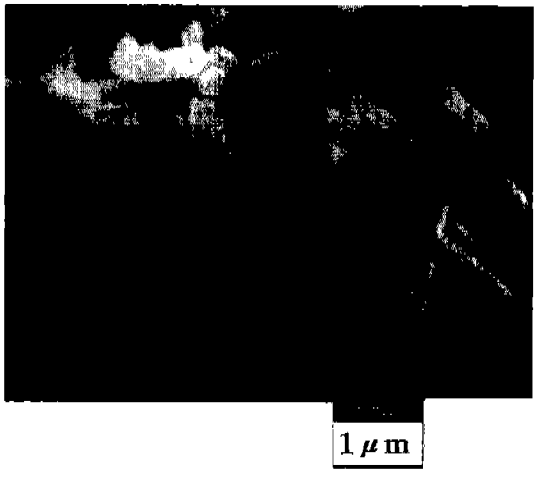

Fig. 6. SEM Micrograph of fracture surface of samples fabricated with alumina-25 wt.% boron oxide after firing at 800℃.

as the firing temperature increases up to 1,100℃. For a firing temperature 1,200℃, another aluminum borate ($9Al_2O_3 \cdot 2B_2O_3$) whisker forms by the reaction of alumina and aluminum borate ($2Al_2O_3 \cdot B_2O_3$),[17]

$$2(2Al_2O_3 \cdot B_2O_3)+5Al_2O_3 \rightarrow 9Al_2O_3 \cdot 2B_2O_3(Al_{18}B_4O_{33}) \quad (2)$$

The bend strength of samples fired at 1,300℃, and 1,500℃ decreased due to loss of structural integrity resulting form the vaporization of excess B_2O_3 component after the formation of $9Al_2O_3 \cdot 2B_2O_3$.[18] Below 1,300℃, secondary heat treatments increased the density, whereas above 1,300℃, fired density was lower than the green density due to the increase of porosity associated with the vaporization of excess B_2O_3. Moreover, the morphology of the aluminum borate ($9Al_2O_3 \cdot 2B_2O_3$) whisker became distinct as the temperature increased as revealed by SEM. This was expected to be due to the vaporization with increasing firing temperature of excess boron oxide that covers the spaces between $9Al_2O_3 \cdot 2B_2O_3$ whiskers.

Comparison of the fracture surfaces of test bars by SEM both before and after infiltration suggests a significant increase in density after infiltration with colloidal silica and firing at 1,600℃ (Fig. 7). Accordingly, the apparent density was found to increase from 1.05 to 1.98 g/cm^3 after second infiltration and firing (about 75% of theoretical density). However, the porosity between layers still exists (Fig. 7 (c)). Four-point bend testing of these test bars after second infiltration resulted in an average bend strength of about 33 MPa (4.8 ksi). The crystalline phase after first infiltration and heat treatment at 1,600℃ was identified to be mullite ($3Al_2O_3 \cdot 2SiO_2$) (Fig. 8). This was due to the reaction of alumina with infiltrated silica as is shown in

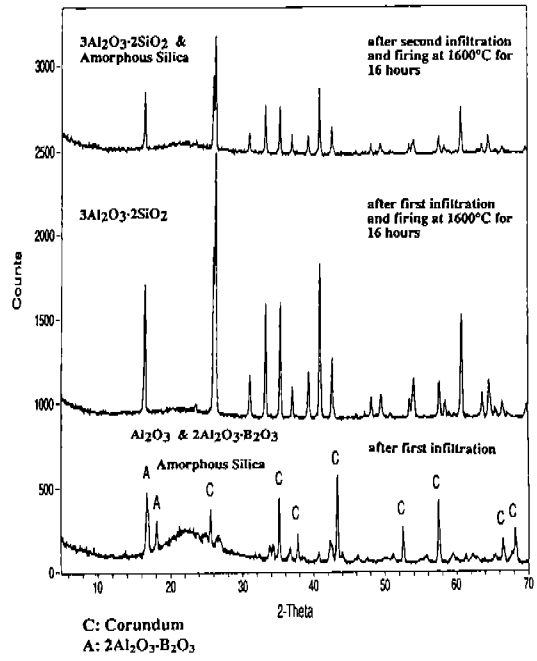

Fig. 8. X-ray diffraction analysis of test coupons infiltrated with colloidal silica.

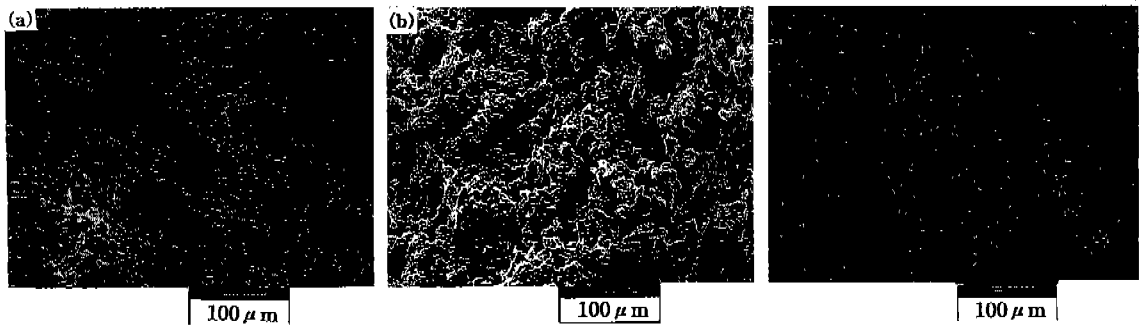

Fig 7. SEM micrographs of fracture surface of test bars fabricated with alumina-25 wt.% boron oxide powder blend followed by firing at 900℃ for 6 hours and infiltration with colloidal silica : (a) before infiltration, (b) after first infiltration with colloidal silica and heat treatment at 1,600℃ for 16 hours, (c) after second infiltration and firing at 1,600℃ for 16 hours.

Equation 3,

$$3Al_2O_3+2SiO_2 \rightarrow 3Al_2O_3 \cdot 2SiO_2 \quad (3)$$

After a second infiltration and heat treatment, it was found that neither the conversion of the incorporated amorphous silica phase into the mullite phase nor the crystallization of the silica phase took place. It was obvious that there was insufficient amount of alumina to react with the silica in the sample. However, there are no good explanations of why the transformation of the amorphous silica phase into the crystalline silica phase such as tridymite does not take place. Further study should be required to investigate above results. According to Inductively Coupled Plasma Atomic Emission Spectroscopy (ICP-AES) data, the remaining boron content after second infiltration and heat-treatment is only about 0.5 wt.%. This suggests that the vaporization of boron oxide at the firing temperature 1,600℃ is quite significant. Therefore, it is expected that there is no chance of the formation of SiO_2 and B_2O_3 compound. It was found that there were only negligible dimensional changes during the course of infiltration and subsequent firing. This suggests that the infiltrants fill the parts and help to increase the density.

The X-ray diffraction patterns of the chromic acid infiltrated test bar (Fig. 9 (a)) reveal that liquid chromic acid (H_2CrO_4) is transformed to chromium trioxide (CrO_3) after drying at 120℃ in a drying oven for several hours. Subsequent heat treatment at 900℃ for 2 hours in air converts the chromium trioxide CrO_3 to chromium sesquioxide Cr_2O_3 (Fig. 9 (b)). This process of infiltration followed by drying and heat treatment at 900℃ were repeated until saturation was achieved. The infiltrated chromium oxide is becoming dominant relative to alumina and aluminum borate as the number of infiltration increases (Fig. 9 (c)). After a final heat-treatment at 1,600℃ for 16 hours, Cr_2O_3 and Al_2O_3 form solid solution as revealed by X-ray diffraction (Fig. 9 (d)). Both Cr_2O_3 and Al_2O_3 have the same corundum

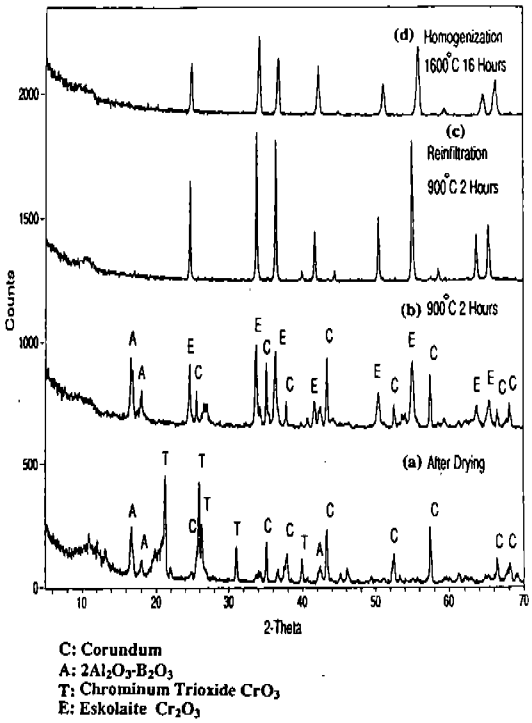

Fig. 9. X-ray diffraction analysis of test coupons infiltrated with chromic acid at different stages.

structure and reflections corresponding to the solid solution occur in positions located between those expected for pure Cr_2O_3 and Al_2O_3. This is due to a slight difference in the ionic radii[15] of Al^{3+} (0.67Å) and Cr^{3+} (0.76Å) and is in accordance with the phase diagram.[19]

Fig. 10 shows the fracture surfaces of the samples infiltrated with chromic acid. Fig. 10 (a) illustrates the ultrafine grained Cr_2O_3 with an average grain size of 0.5 μm that was obtained after firing at 900℃. The shape of the grains is spherical. After the homogenization process at 1,600℃ for 16 hours, the size of the spherical grains increases significantly (Fig. 10 (b)). The crystal structure of these grains was identified as a solid solution of Al_2O_3-Cr_2O_3. The apparent density of test bar increased from 1.05 g/cm^3 to 2.6 g/cm^3 after first homogenization. After the second infiltration and homogenization, the infiltrated powder particles incorporated into spherical grains, resulting in a continuous po-

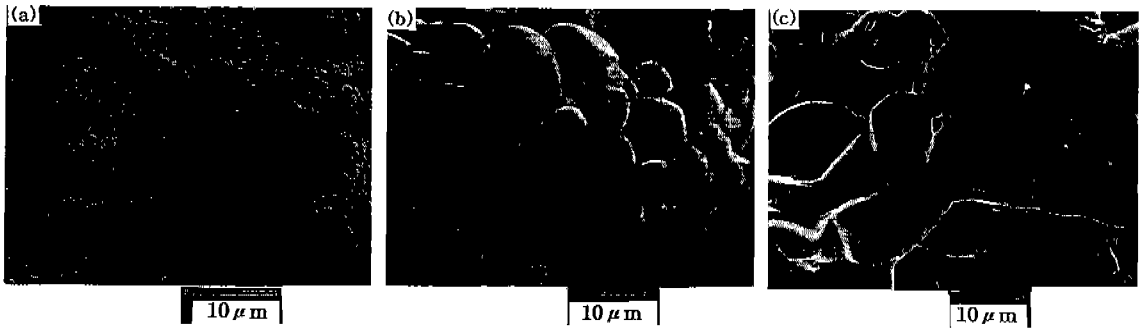

Fig. 10. SEM micrographs of fracture surface of test bars infiltrated with chromic acid : (a) after first infiltration, (b) after first infiltration and homogenization, (c) after second infiltration and homogenization.

lycrystalline material (Fig. 10 (c)) and the density of the test bar increased significantly. The density of samples increased to 4.03 g/cm^3 (about 80% of theoretical density) and the four-point bend strength reached about 15 MPa, which was much lower than that of the samples infiltrated with colloidal silica. It appeared that the mullite phase is much stronger than the Cr_2O_3 dominant solid solution of Al_2O_3-Cr_2O_3. It was also found that there were no dimensional changes of test bars during infiltration process as in the case of silica infiltration.

4. Conclusions

It has been shown that monoclinic HBO_2 is a potentially useful inorganic binder for SLS of alumina to obtain structurally sound parts. It was also demonstrated that both a composite body Al_2O_3-$2Al_2O_3 \cdot B_2O_3$ and a monolithic material $9Al_2O_3 \cdot 2B_2O_3$ could be successfully fabricated by selective laser sintering and reactive sintering of the material system Al_2O_3-B_2O_3. The bend strength of the composite body increased as the binder content increased. At higher laser energy density, the composites showed higher bend strength due to higher density. For intermediate firing temperatures around 800~1,100℃, test bars showed higher bend strength due to the formation of whisker-like aluminum borate ($2Al_2O_3 \cdot B_2O_3$) grains at the surface of the alumina particles by the reaction of alumina and boron oxide. For a firing temperature of 1,200℃, single phase $9Al_2O_3 \cdot 2B_2O_3$, which has a whisker structure was formed by the reaction,

$$2(Al_2O_3 \cdot B_2O_3)+5Al_2O_3 \rightarrow 9Al_2O_3 \cdot 2B_2O_3 \quad (4)$$

The morphology of the aluminum borate ($9Al_2O_3 \cdot 2B_2O_3$) whisker became distinct as the firing temperature increased due to the vaporization, with the increase of firing temperature, of excess boron oxide, which covers spaces between $9Al_2O_3 \cdot 2B_2O_3$ whiskers.

The infiltration technique was an effective way to partially densify alumina-aluminum borate ($2Al_2O_3 \cdot B_2O_3$) composites, which were fabricated by firing at 900℃ for 6 hours of green SLS parts obtained from alumina-monoclinic HBO_2 powder blends. Between the two infiltrants selected, the performance of colloidal silica as an infiltrant was found to be better by the evaluation in terms of density and bend strength of the composites. This was due to the formation of mullite ($3Al_2O_3 \cdot 2SiO_2$), which is an excellent high-temperature structural material, by the reaction of alumina with infiltrated silica. The maximum density of the composite after infiltration with colloidal silica and firing was about 75% of theoretical density and the maximum bend strength was increased from 8 MPa to around 33 MPa. The infiltration with chromic acid into this composites yielded a solid solution of Al_2O_3-Cr_2O_3 whose density was about 80% of the theoretical density and the bend strength was around 15 MPa.

References

1. H. L. Marcus, J. J. Beaman, J. W. Barlow, and D. L. Bourell: Journal of Metals **42** (1990) 8.
2. J. J. Beamam, Design News **46**(3) (1990) 65.
3. J. C. Nelson, Selective Laser Sintering: A Definition of the Process and an Empirical Sintering Model, Ph. D. Dissertation, University of Texas at Austin, Austin, Texas (1993).
4. D. Kochan: Solid Freeform Manufacturing, Elsevier, New York (1993) 93.
5. Insup Lee, A. Manthiram, and H. L. Marcus: Proceedings of the Solid Freeform Fabrication Symposium, **5** (1994) 339.
6. U. Lakshminarayn: Selective Laser Sintering of Ceramics, Ph.D. Dissertation, University of Texas at Austin, Austin, Texas (1992).
7. K. Subramannian, G. Zong, and H. L. Marcus: Proceedings of the Solid Freeform Fabrication Symposium, **3** (1992) 63.
8. R. M. German: Liquid Phase Sintering, Plenum Press, New York and London (1989) 17.
9. P. Hasse: Selective Laser Sintering of Metal Powders, M.S. Thesis, University of Texas at Austin, Austin, Texas (1989).
10. D. L. Bourell, H. L. Marcus, J. W. Barlow, and J. J. Beaman: Int. J. Powder Met. **28**(4) (1992) 369.
11. N. N. Greenwood, A. Earnshow: Chemistry of the elements, Pergamon Press, Oxford (1984) 228.
12. R. H. Doremus, Glass Science, John Wiley & Sons, Inc., New York (1973) 20.
13. R. S. Roth, J. R. Dennis, and H. F. McMurdie: Phase Diagrams for Ceramists, American Ceramic Society Inc., Columbus (1987) 141.
14. N. K. Vail and J. W. Barlow: Proceedings of the Solid Freeform Fabrication Symposium, **3** (1992) 124.
15. D. W. Richerson: Modern Ceramic Engineering, Marcel Dekker, Inc., New York (1992) 588.
16. B. R. Marple and D. J. Green: Commun. Amer. Ceram. Soc., **71**, (1988) C-471.
17. S. P. Ray: J. Amer. Ceram. Soc., **75**(9) (1992) 2605.
18. K. Okada, H. Mutoh, N. Otsuka, and Y. Yano: J. Mater. Sci. Lett., **10** (1991) 588.
19. Phase Diagrams for Ceramists, Vol. 1, American Ceramic Society, Columbus, Ohio (1964) 121.